We are IntechOpen, the world's leading publisher of Open Access books Built by scientists, for scientists

4,800
Open access books available

122,000
International authors and editors

135M
Downloads

Our authors are among the

154
Countries delivered to

TOP 1%
most cited scientists

12.2%
Contributors from top 500 universities

CLARIVATE ANALYTICS BOOK CITATION INDEX INDEXED

WEB OF SCIENCE™

Selection of our books indexed in the Book Citation Index in Web of Science™ Core Collection (BKCI)

Interested in publishing with us?
Contact book.department@intechopen.com

Numbers displayed above are based on latest data collected.
For more information visit www.intechopen.com

9

Mesostructured Polymer Materials Based on Bicontinuous Microemulsions

Masashi Kunitake[1,2*], Kouhei Sakata[1] and Taisei Nishimi[3]
[1]*Graduate School of Science and Technology, Kumamoto University, Kurokami, Kumamoto*
[2]*Core Research for Evolutional Science and Technology*
Japan Science and Technology Agency (JST-CREST), Honcho, Kawaguchi, Saitama
[3]*FUJIFILM Corporation, Kaisei-machi, Ashigarakami-gun*
Japan

1. Introduction

A bicontinuous microemulsion (BME, Winsor III), also called a middle-phase microemulsion, is a low-viscosity, isotropic, thermodynamically stable, spontaneously formed solution phase composed of water, organic solvent, and surfactants. The dynamic morphology of a microemulsion (ME) is generally determined by the hydrophilicity–lipophilicity balance (HLB) of the surfactants in the emulsion system, as shown in Figure 1. When the hydrophilicity and lipophilicity of a surfactant are well balanced in an ME system, the ME frequently possesses a bicontinuous structure, in which the water phase and the oil phase coexist on a microscopic scale. In this chapter, polymer materials prepared from BMEs are introduced. Unique polymer morphologies such as continuous porous monolithic, bicontinuous hybrid, and nanosheet structures were prepared by polymerization or gelation in BMEs.

Polymer emulsion or ME systems have a wide range of industrial applications, e.g., in adhesives, paints, paper coating and textile coatings. Emulsions are widely used in the production of polymer materials, especially polymer particles. Most polymer particles are formed by suspension or emulsion[1,2] polymerization. Recently, surfactant-free polymerization, so-called soap-free polymerization, using an ionic radical initiator in aqueous solvents, homogeneous polymerization, dispersion polymerization,[3-9] and precipitation polymerization[10,11] have become popular because the polymer products are surfactant-free.

Methods of forming monolithic bulk polymer products with continuous pores, based on spinodal decomposition processes, have been researched intensively; a major advantage of monolithic supports is that mass transfer can take place through their pores. Porous polymer monoliths first emerged as a new class of stationary phases for high-performance liquid chromatography in the early 1990s after the development of inorganic monoliths prepared from silica using a sol–gel reaction.[12] The spinodal decomposition method has also

* Corresponding Author

been used for control of pore structures in commercial filters; this is a very important industrial application. These monoliths are typically prepared from a mixture comprising monomers, an initiator, and a porogenic solvent, using a simple molding process carried out in a mold such as a tube or a capillary. [13] Methods using spinodal decomposition have been used to prepare polymer membranes for separation. Polyether sulfone porous membranes have an asymmetric structure, leading to good permeation performance. Membranes prepared by these methods are commercially available. [14] Kumar and coworkers produced monolithic columns consisting of porous polyacrylamide, and they reported that the polymer columns were effective as affinity-chromatography supports for cell separation. [15]

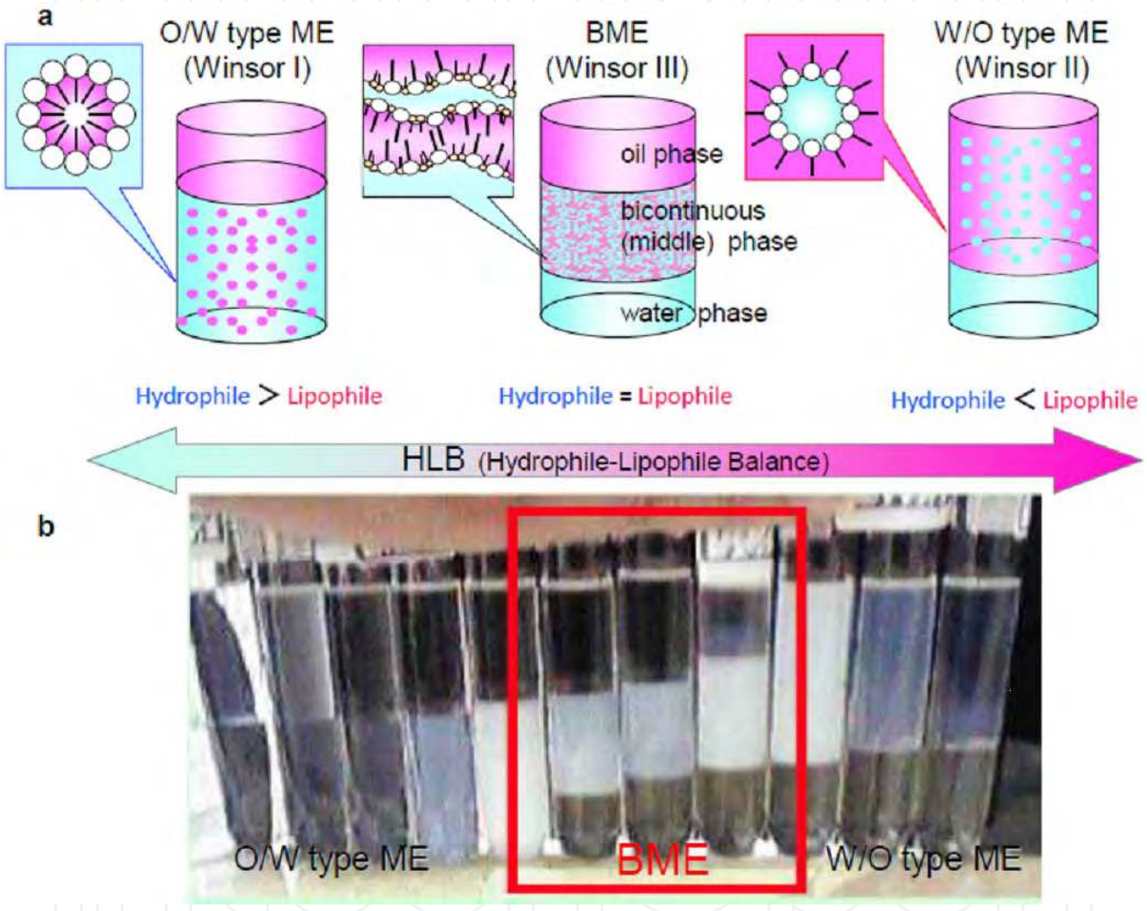

Fig. 1. Schematic representation and corresponding photographs of a series of MEs controlled by HLB (a, three types of ME model; b, functional ME (toluene/SDS + 1-butanol/saline). The phase structures of MEs were controlled by saline concentration.

Continuous porous polymer materials (molded monolithic porous polymers) can also be produced by decomposition of one component from a bicontinuous "gyroid" block-copolymer structure. Hashimoto and coworkers succeeded in obtaining continuous porous polystyrene (PS) with pores of diameter several tens of nanometers by dismantling polyisoprene by selective decomposition with ozone after having formed bicontinuous structures using PS/polyisoprene or polyisoprene/poly(2-vinylpyridine) block copolymers. [16,17] As described below, spinodal decomposition should be considered for BME polymerizations. It is worth

noting that BMEs and spinodal-decomposition structures possess essentially the same "sponge-like" structure and that the only difference between them is size. Hashimoto and coworkers have summarized the associated theories on a physicochemical basis.

2. Construction of continuous porous polymer materials by BME polymerization

Thermal polymerization of BMEs consisting of a monomer liquid (oil) and water with an initiator is the simplest way to immobilize a BME structure. Simple BME polymerization leads to formation of continuous porous structures based on a bicontinuous-solution structure. In 1988, Haque and Qutubuddin reported the first preparation of porous PS based on a BME (styrene + 2-pentanol/SDS/water).[18]

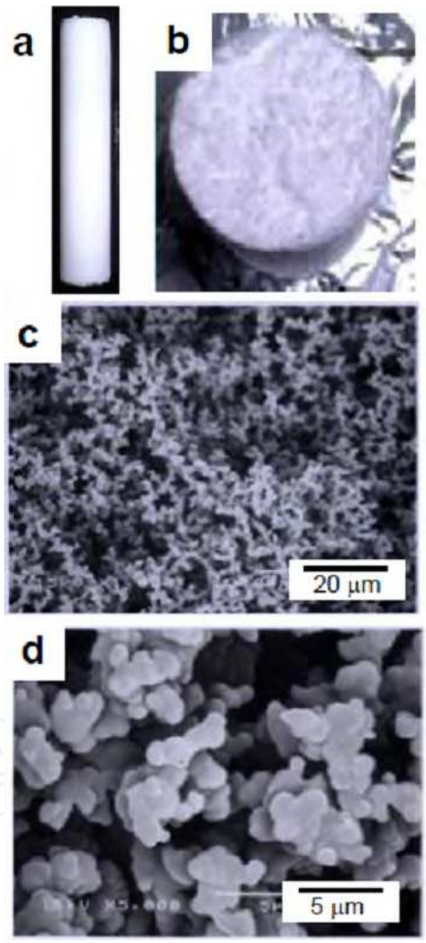

Fig. 2. Typical photographs (a, outer surface; b, torn surface) and SEM images (c and d) of the PS product prepared by BME thermal polymerization (styrene/SDS + 1-butanol/saline solution) in a glass tube.

We conducted a similar thermal polymerization of styrene/SDS + 1-butanol/saline solution; the HLB was controlled by the cosurfactant and salt concentrations. A hard white cylinder (Figure 2a) with a porous structure was formed. A porous structure was clearly observed in

scanning electron microscopy (SEM) images, as shown in Figure 2c and d. The observed network structure consisted of connected particles, indicating percolation. When the BME polymerization was conducted using a BME solution in which two electrodes were separately placed, the electroconductivity of the polymer product was similar to that before polymerization, indicating the presence of a continuous micro saline-phase. However, the obtained pore size was 10 times larger than that expected, based on the solution structure. BME solution thicknesses have been determined using small-angle neutron scattering,[19] transmission electron microscopy with a freeze-fracture replica technique,[20,21] and simulations.[22] The reported thicknesses were from several tens of nanometers to 100 nm, and depended on the emulsion system and the measurement method. Transmission electron microscopy observation of a freeze-fracture replica sample has been used as a direct visual method. Abe and coworkers observed typical textures with thicknesses less than 100 nm for polymeric silicone BME systems.[20]

Continuous increases in pore sizes and polymer-wall thicknesses are generally observed as BME polymerization progresses. This phenomenon is the result of phase separation induced by a shift in the HLB equilibrium during polymerization. This phase separation is essentially the same as spinodal decomposition from the liquid phase. The driving force of this phase separation is a decreasing affinity of the surfactant for the oil phase consisting of monomer and newly formed polymer. This was proved by the appearance of an oil/water phase when PS was added to a styrene BME solution. The nano/meso-structures of chemically immobilized BME polymers are therefore predominantly determined by competitive reactions between immobilization and meso-phase separation during polymerization. In other words, the pore size should be controlled by the polymerization speed.

The production of porous structures with submicron continuous pores has been a goal since research in the field of BME polymerization began. Such products are expected to be transparent polymers with continuous pores. In order to construct such polymer products, polymerization-induced phase-separation should be avoided and/or suppressed. Generally, the meso-structures of polymer products prepared by BME polymerization are regulated kinetically by the competitive relation between immobilization by polymer growth and meso-phase separation. In order to achieve this, acceleration of immobilization (polymerization) and inhibition of phase separation are crucial. The immobilization speed should be increased. Increasing the initiator concentration and introduction of cross-linking agents are advantageous in terms of immobilization speed. It is worth noting that the polymerization temperature involves a trade-off because the speeds of both immobilization and phase separation increase with increasing temperature. Photo-induced polymerization at relatively low temperatures is therefore frequently used to suppress phase separation.

The most efficient approach will involve the use of polymerizable surfactants. The immobilization of polymerizable surfactants located at saline/oil interfaces is highly effective in suppressing the phase separation induced by polymerization. Transparent polymer products with continuous pores of diameter with several hundred nanometers or less are produced by polymerization of polymerizable surfactants and/or monomer (oil) phases.

Gan and coworkers[23] reported photopolymerization of the BME system (methyl methacrylate (MMA) and (2-hydroxyethyl) methacrylic acid (HEMA) mixed monomer solvent (1:1) /polymerizable cationic surfactant/water). They confirmed BME conditions of their system from the solution transparency and electroconductivity. Since the late 20th century,

nanostructured proton-exchange membranes prepared by photopolymerizing BMEs have been a focus of attention because of their potential use in fuel cells. The continuous pores in membranes possess ionic passages. The inherent BME structure is essentially transferred to the matrix of the polymer membrane, without obvious phase separation, by polymerization. Gan[24] also reported photopolymerization of the BME solutions MMA/3-[(11-acryloyloxyundecyl)imidazoyl]propyl sulfonate (AIPS)/water, conducted between glass plates, to prepare transparent porous polymer membranes (Figure 3). The transparent membranes possessed proton-exchange properties as a result of introduction of a polymerizable zwitterionic surfactant. They reported continuous pores (channels) on the 20–50-nm scale. Liu et al.[25] reported the synthesis proton-exchange membranes with nanopores (diameter 1.5–2 nm) by thin-layer photopolymerization in a BME solution system (acrylonitrile/AIPS + cosurfactant/water). The pore scale is smaller than expected based on the size of the water channels in the BME solution before polymerization. Yang and coworkers[26] developed transparent, nanostructured, NIPAAm-based thermosensitive polymer membranes prepared from a BME system.

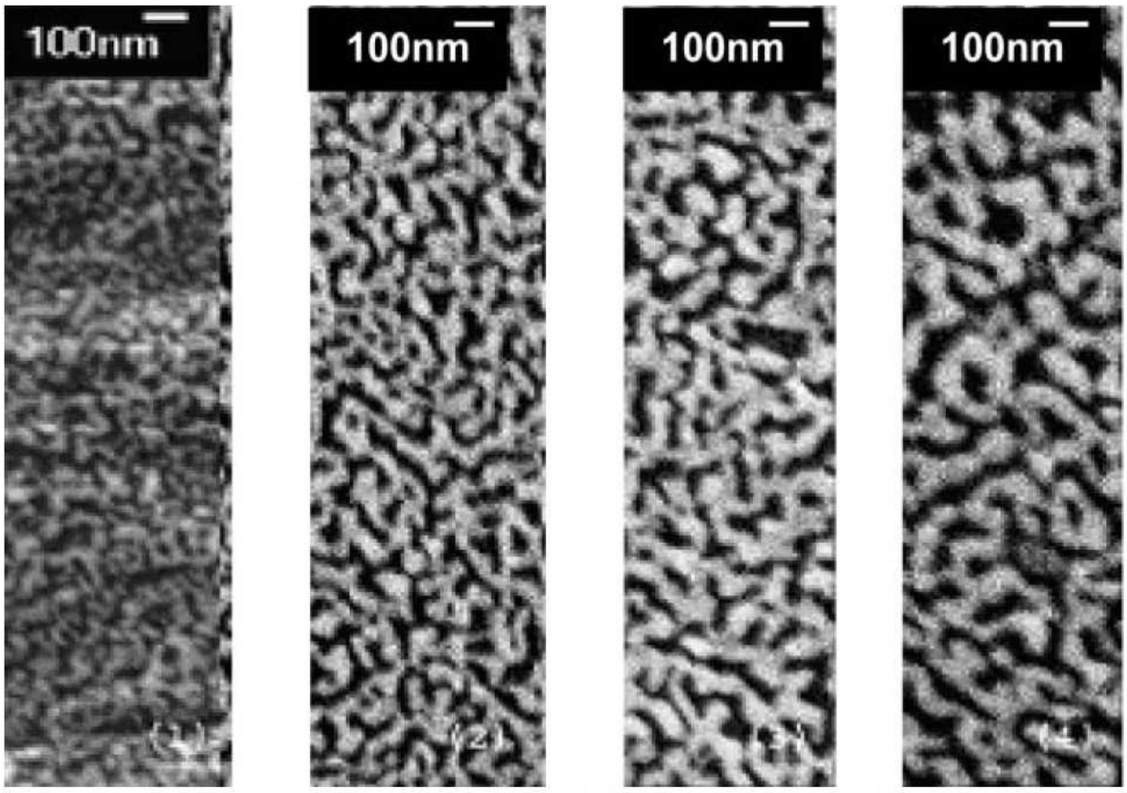

Fig. 3. SEM images of porous membranes prepared by polymerization with a polymerizable zwitterionic surfactant, AIPS (35 wt%), MMA (35 wt%), and water (30 wt%).[24]

3. Construction of hybrid soft materials by BME gelation

BMEs are used to produce not only porous condensed polymer products but also a new class of unique soft gels. Soft materials (soft matter), which are easily deformed, are

important in a wide range of technological applications. Stimuli-responsive (intelligent) gels,[28] double-network (DN) gels,[29] nanocomposite gels,[30] and topological gels[31] have been extensively researched in the past decade. Such gels are expected to have potential as polymer materials for actuators[32] and drug-release systems;[33] these are key polymer technologies of the future.

Soft "wet" gels are categorized as organogels or hydrogels, according to the solvent used, which is a major component of the gels in terms of weight fraction. Generally, organogels and hydrogels are prepared by gelation to form three-dimensional networks based on physical aggregation (physical gelation) or chemical polymerization with cross-linking (chemical gelation). Gelation in emulsions or MEs has been investigated for composite gel formation since the 1980s.[34] Hydrogel particles prepared by hydrogelation in water/oil (W/O) emulsions have been investigated.[35] Bulk organogels bearing water microdroplets, prepared by organogelation in W/O emulsions, have also been investigated because of their medical applications such as dermal drug-delivery.[36] As expected, the converse combinations are possible but have rarely been reported.[37]

We have conducted gelation in BMEs (toluene/SDS and cosurfactants/saline) to produce hydro-organogels. Organogelation and hydrogelation were respectively achieved by physical gelation with an organogelator, namely 11-hydroxystearic acid, and polymerization (chemical gelation) of acrylamide with a cross-linker. Then, three composite gel systems, namely a BME organogel, a BME hydrogel, and an organo/hydro hybrid BME gel, were produced by hydrogelation and/or organogelation of each solution phase.

Figure 4 shows typical products obtained by gelation of macroscopic three-phase solutions including a BME phase. The BME phase (a middle-phase ME) is the middle phase of the macroscopic three-phase solutions. The upper and lower phases are a toluene phase and an aqueous phase, respectively. These gels, i.e., a BME organogel, BME hydrogel, and an organo/hydro hybrid BME gel, were self-supporting and very soft and elastic. Even in "one-side only" gelation products such as the BME organogel and the BME hydrogel, the solvent phases without a gelator were also macroscopically immobilized. No macroscopic pores were observed for any of the three BME gels. Moreover, all the BME gels had ionic conductivity, proving that the aqueous phase was continuous and that the bicontinuous structure was retained in the composite gels.

SEM images of freeze-dried one-side-gelated BME samples, i.e., the BME organogel and BME hydrogel, had uniform sponge-like porous structures, as shown in Figures 4h–k. The walls of the porous structures consisted of fiber networks, which were essentially similar to those in bulk organogels or hydrogels. In contrast, the morphology of the both-sides-gelated BME organo/hydro hybrid gel was entirely different, with a pore-free and smooth surface (Figure 4k).

In the case of soft swelling gels, a dried sample is necessary for SEM observations, and it is very difficult to eliminate the influence of the drying process on the structural analysis, even if the SEM sample is prepared by freeze-drying to minimize such influences.

In-situ imaging of "wet" BME gels was conducted using confocal laser scanning microscopy (CLSM). CLSM is a powerful nondestructive monitoring tool that provides three-dimensional mapping at the submicron scale by discrimination between the saline

phase and oil phase under wet conditions.[38] By using hydrophilic and lipophilic fluorescent dyes, the aqueous region, oil region, and well-mixed region can be distinguished as different colors on the submicron scale. In Figures 4d–g, the red and green areas indicate phase-separated regions for the saline and toluene micro-phases, respectively. The yellowish color indicates that both oil and saline phases were uniformly mixed on a submicron scale. Because of the resolution limit, phase separation in BME gels cannot be estimated below 100 nm by CLSM.

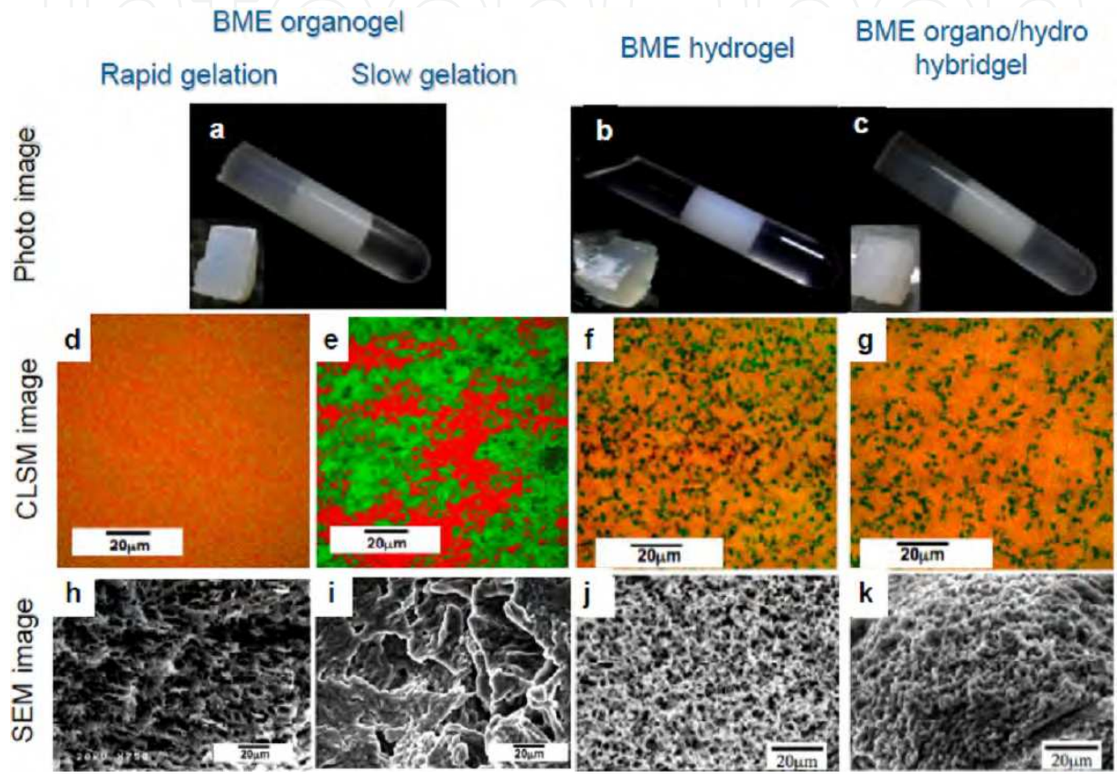

Fig. 4. Photographs (a–c), CLSM images (d–g), and SEM images (h – k) of a BME organogel (a, d, e, h, and i), BME hydrogel (b, f, and j), and BME organo/hydro hybrid gel (c, g, and k). The BME organogels were produced by "rapid" (d and h) and "slow" (e and i) cooling.[27]

The structures of BME gels are influenced by the kinetics of the gelation process, rather than by thermodynamic control of the original BME solution structure; this is similar to the case of condensed gels prepared by BME polymerization. Kinetic control of the physical gelation process to produce BME organogels was achieved relatively simply by control of the rate of cooling from the "sol state" to the "gel state". The BME organogel prepared by "rapid gelation" cooling (Figure 4d) gave a well-mixed submicron-scale BME gel (a texture-less yellowish color). This clearly proved that "rapid gelation" achieved immobilization of the solution structure in BME at less than several hundred nanometers, although even the microstructure of a gel prepared by "rapid" cooling might be influenced by mesoscopic phase-separation. In contrast, "slow" gelation cooling, typically at ca. 0.3 °C min^{-1} from 60 to 5 °C, provided a mosaic pattern consisting of two large domains, distinguished as green and red, indicating mesoscopic phase-separation (Figure 4e). The aqueous regions and oil

regions were separated bicontinuously on a scale of several tens of microns, and no yellowish region was observed.

Generally, mesostructures are regulated by a competitive relationship between gelation speed and meso-phase separation speed. The driving force of mesoscopic phase-separation is the lowering of the surfactant activity by gelation. The propagation of gel fibers in oil or aqueous micro-phases kinetically induces lowering of the surfactant activity following mesoscopic phase-separation, in which the aqueous and oil phases progressively separate.[39] The mesoscopic phase-separation mechanism is similar to that of spinodal decomposition from the viewpoint of kinetic control.

Similar to the situation for BME organogels prepared by physical gelation, chemical hydrogelation in BME, namely polymerization of acrylamide with N,N′-methylene bisacrylamide, allowed us to produce bicontinuous composite gels. Jinnai and coworkers have reported porous NIPAAm polymer gels prepared by spinodal decomposition.[38,40] In the case of chemical gelation, the mesostructures are also kinetically regulated by gelation speed. It is well known that the use of a chemical accelerator, tetramethylethylenediamine (TEMED), increases gelation speed significantly.

However, the use of an accelerator represents a trade-off in terms of pore size because immobilization of the BME solution starts immediately on addition of TEMED to the BME solution, before the emulsion system can reach thermodynamic equilibrium. The ME system needs a standing time to reach a true thermodynamic equilibrium. Even when the solution seems to be macroscopically homogeneous, the thickness of the liquid layer of the bicontinuous phase changes continuously toward an equilibrium state after mixing. For instance, when the BME hydrogel was prepared by "rapid" gelation with TEMED without considering the stabilization time, the reaction started instantly and gelation was complete in less than 15 min. The CLSM image (Figure 4g) reveals the formation of a homogeneous bicontinuous structure consisting of isolated micron-scale green and red regions. There was almost no yellowish region, and the green and red regions did not overlap on the CLSM scale. In addition, it was possible to control the pore and wall sizes of the bicontinuous texture, which was on a scale between submicron and several tens of microns, by the reaction temperature.

By means of double gelation in oil and saline micro-phases, bicontinuous organo/hydro hybrid gels, in which the both the organic and aqueous micro-phases were immobilized, were produced as novel hybrid soft gels. Gong and coworkers reported DN hydrogel systems that were very tough and showed low friction, and discussed the similarities of these DN gels to biosystems.[39] The structure of the BME hybrid gel consisted of a homogeneous BME gel phase (yellowish) and separated islands (green), as shown in Figure 4f. The texture in the CLSM image was very similar to that of the BME hydrogel. As hydro chemical gelation was conducted prior to organo physical gelation, the mesostructure of the hybrid gels was predominantly determined by the hydrogelation step.

The hierarchical structures of polymer products (including soft gels) produced from BMEs were regulated by competition between three synergetic rate factors, namely immobilization of the BME structure by gelation, mesoscopic phase-separation by gelation, and time-dependent transformation of the solution/solution structure toward a thermodynamic structure in the equilibrium state.

4. Determination of BME solution structures at solid/liquid interfaces by electrochemical analysis

BME nanostructures are also attractive as media for electrochemical studies.[42,43] Rusling et al. conducted pioneering work on the electrochemistry of BME solutions using a glassy carbon (GC) electrode.[44] The electrochemical approach to BMEs shows the dynamic solution structure of BMEs at solid/liquid interfaces. The electrochemistry of redox molecules, namely $K_3Fe(CN)_6$ and ferrocene, in a BME (saline/SDS + butanol/toluene) was investigated in detail using various electrodes such as indium tin oxide (ITO), Au disk, GC disk, highly oriented pyrolytic graphite (HOPG), and alkanethiol-modified Au electrodes (Figure 5). The electrochemical contact with the micro aqueous and organic solution phases in a BME is alternately or simultaneously achieved by controlling the hydrophilicity and lipophilicity of the electrode surfaces.[45,46]

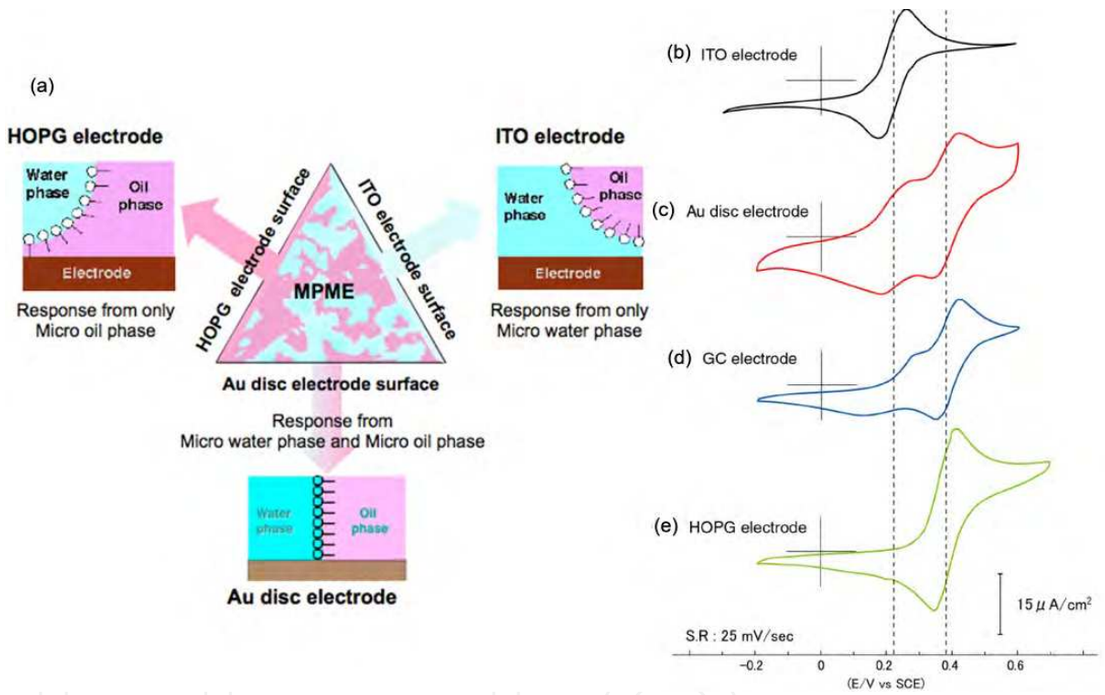

Fig. 5. Schematic representation of BME solution structures at solid/oil/saline interfaces (a) and typical cyclic voltammograms measured using ITO (b), polished Au disk (c), polished GC (d), and cleaved HOPG (e) electrodes in BME in the presence of $K_3Fe(CN)_6$ and ferrocene.[41]

The amphiphilic electrode (Au) revealed redox peak couples for both $K_3Fe(CN)_6$ and ferrocene in BME solutions simultaneously.[45] In contrast, strong hydrophilic or lipophilic electrodes (ITO and HOPG) produced only one of the peak couples of $K_3Fe(CN)_6$ or ferrocene, depending on the affinities for the detecting electrodes. For instance, an ITO electrode possesses a strongly hydrophilic, negatively charged surface. No redox peaks resulting from ferrocene in a micro oil-phase were observed, although the redox peaks of $K_3Fe(CN)_6$ in a micro saline-phase were clearly observed. Conversely, strongly lipophilic (hydrophobic) electrodes such as HOPG, with a neutral surface, showed the opposite electrochemical response in the BME.

The solution structure of a BME around the electrode changes thermodynamically in response to the HLB of the electrode surfaces. A well-balanced BME solution structure is easily converted to a biased or one-sided structure on an electrode surface to minimize surface energy. As mentioned already, the unique characteristics and structures of BMEs are based on the very delicate balance between the hydrophilicity and lipophilicity of the surfactant system; this balance is moderated by the concentrations of the cosurfactant and salt, or by the temperature.

It is worth emphasizing that an electrochemical response of the redox species in the micro toluene phase in a BME was observed even if there was no electrolyte in toluene phase . This indicates that the ionic conductivity is maintained via a continuous saline phase in the BME; this phase acts as an ion-conducting passage. This suggests that electrochemistry in nonpolar solvents without an electrolyte, becomes possible in BMEs.

These alternative electrochemical responses in BMEs indicate that the bulk bicontinuous structure is thermodynamically discontinuous near the surface, as a result of the influence of the hydrophilicity or lipophilicity of the electrode surface. Hydrophilic and lipophilic (hydrophobic) surfaces predominantly face the micro saline-phase and the micro organic-solvent phase, respectively, in BMEs.

The dynamic solution structures of three-phase interfaces (oil/water/solid) of BMEs have been discussed in terms of the apparent diffusion coefficients (D_{app}) of each redox species and electrode. Despite the complex solution structures, the scan-rate dependence of the peak currents for $K_3Fe(CN)_6$ and ferrocene in the BME indicated that the system is generally regulated by relatively simple diffusion control. The D_{app} for each redox species is calculated from the scan-rate dependence of the peak currents according to the Randles–Ševčik equation.

Lindman and coworkers reported that the self-diffusion coefficients of both solution species, water and toluene molecules, in the BME solutions, which were obtained by Fourier-transform pulsed-gradient spin-echo NMR measurements, were slightly smaller than those in homogeneous solutions.[47] In principle, the diffusion coefficients in a homogeneous solution should be independent of the type of electrode. However, the D_{app} values obtained using the hydrophilic ITO and lipophilic pyrolytic graphite (PG-b) electrodes were less than half of those obtained with the amphiphilic Au electrode. The ratios of the D_{app} values of ferrocene for Au against those for PG-b in the BME decreased with increasing temperature. Such deviations of D_{app} values from the ideal values provide information on the solution structure near the electrode surface, and the electrode area in contact with both phases.

These behaviors could not be explained by a simple sloped-structure model because the hydrophilic ITO and lipophilic PG-b electrodes consistently face either the micro saline-phase or the oil-phase, respectively. The results can be explained by an alternating W/O layered structure, as shown in the model (Figure 6).[49-51] The solution layers consist of micro aqueous and micro oil phases that form alternately, starting from the electrode surface. The first solution layer is adopted based on the affinity with the electrode surface. The second, counter-solution layer, either an oil layer or an aqueous layer, forms on the first aqueous or oil layer. The contribution of the layered structure will gradually decrease with increasing distance from the electrode surface. An alternating layered structure causes the lower D_{app} values of the hydrophilic and lipophilic electrodes rather than those of amphiphilic

electrodes. Zhou et al. used small-angle neutron scattering to investigate the alternately layered solution structures of BMEs around solid surfaces.[49-51]

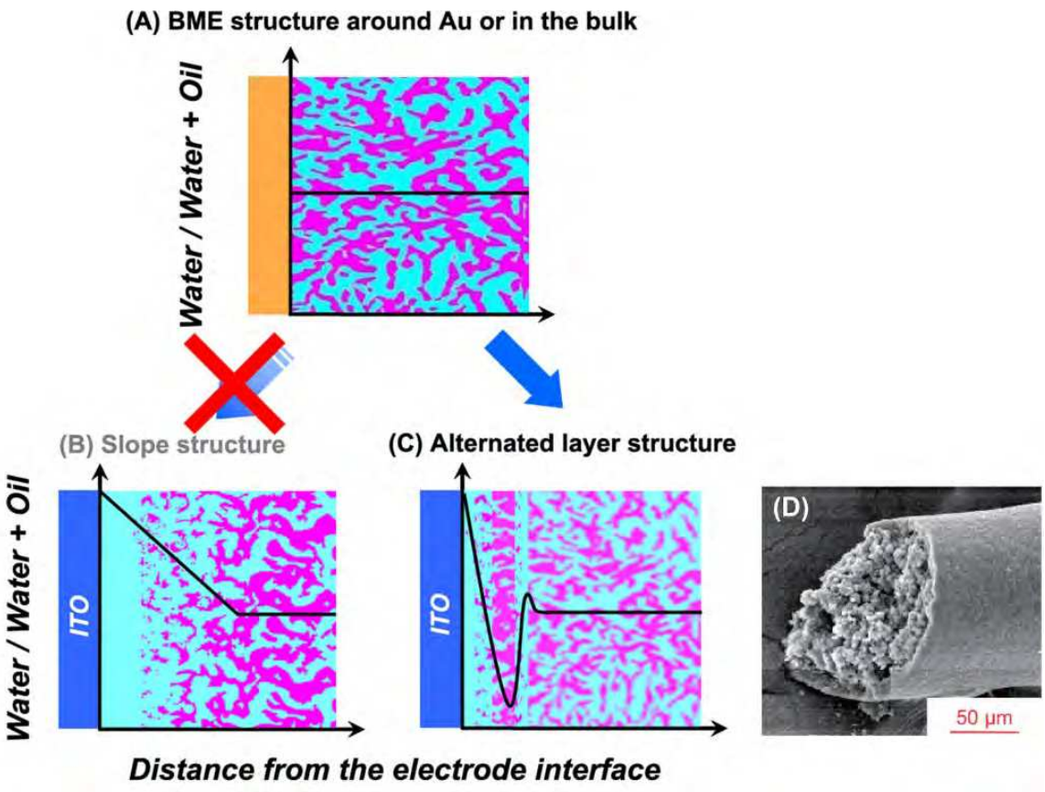

Fig. 6. Schematic illustrations with depth profiles of saline volume ratios for BME structures with bulk and amphiphilic Au electrodes (A), the slope structure (B), and the alternating layered structure around the hydrophilic ITO electrode (C) expected from the apparent diffusion coefficients of redox species and the SEM image (D) of a PS tube with a continuous porous structure and a pore-less surface prepared by thermal polymerization of a styrene BME in a capillary. The magenta and light cyan regions are the oil and saline phases, respectively.[48]

To visually evaluate the influence of the surface on the solution structure of the BME, thermal polymerization of a styrene-based BME was conducted in a capillary glass with an intact hydrophilic surface. The polymer formed in the capillary possessed a typical continuous porous structure based on a granular network, in accordance with that observed for bulk polymerization, and the porous structure was surrounded by a pore-less polymer sheet, as shown in Figure 6D. In addition, a gap between the polymer sheet and the inner wall of the capillary was frequently observed. The pore-less polymer sheets might prove the existence of an alternately layered structure in the BME solution before polymerization.

5. Construction of hierarchical structure based on BMEs and nanospaces

The formation of a polymer tube with continuous pores and seamless walls by simple polymerization in a capillary directed our attention to polymerization of BMEs in other microspaces, such as opal membranes, to construct hierarchical structures. At present,

"structural transcription"[52] from inorganic materials to polymer materials, such as from a "silica opal membrane" to an "inverse opal polymer membrane", is very popular as a method for constructing unique polymer materials with regular, controlled, complex porous structures.[53-55] When thermal polymerization of styrene- or MMA-based BMEs was conducted in the submicron gaps of a silica opal membrane, surprisingly various fractal surface structures consisting of vertical polymer nanosheets were obtained instead of the expected continuous porous PS-filled silica opal membrane. Simple styrene polymerization in the silica opal membrane gave a PS-filled silica opal membrane.

Figure 7 shows typical SEM images of the "turf-like" fractal surface of the opal membrane after polymerization of the styrene BME. Unique morphologies such as fractal surfaces consisting of closely spaced nanosheets and vertically extended nanosheets were grown from the gaps of a silica opal membrane. The surface densities and lengths of the nanosheets were roughly controllable by the polymerization conditions, specifically the thickness of the opal membrane and the amount of BME applied to the membrane. The closely spaced nanosheets were typically ca. 200 nm thick, 0.5–2 μm wide, and 1–4 μm in length. Very long nanosheet ribbons were formed by polymerization in a relatively thick opal membrane (typical thickness > 2 mm). The lengths of the longest nanosheets were several ten of microns; however, the thicknesses and widths were 100 nm and 0.5–4 μm, respectively, almost the same as for nanosheets prepared under different conditions.

Although the concentrations of surfactant, cosurfactant, and salt required to form BMEs were quite different for styrene BMEs and MMA BMEs, the shapes and sizes of the "turf-like" nanosheets of polymethyl methacryrate (PMMA) were very similar to those of the PS nanosheets. These results indicate that the nanosheet structures originate from the solution/solution structure of the BME, regardless of the chemical structures of the monomers.

The nanosheet columns grow from the bottom of the column, not from the apex, analogous to the growth of fingernails. The emulsion species are drawn from the gaps in the opal to the roots of the polymer columns. No polymer species were observed in the silica gaps after polymerization. During the polymerization process, the emulsion, which is a mixture of monomers and polymers (oligomers), escapes through the submicron-scale silica gaps to the surface. The major driving force for escape of ME from the microspace, and the propagation of PS columns, is the lack of stability of the ME solution in the highly hydrophilic microspaces of the silica gaps. Furthermore, the nanosheet structure indicates the existence of a liquid-crystal (LC) phase as a template. Two factors are expected to influence formation of an LC phase from a BME during polymerization. A hydrophilic silica surface tends to trap water near the surface,[45,46] and the decrease in the water content of the ME causes enrichment of surfactants in the ME. The shift of the HLB of the surfactants resulting from the changes in the oil phase of the ME during polymerization, and hence changes in the monomer/polymer ratio and the degree of polymerization, might induce a phase change from a BME phase to an LC phase.

Finally, various fractal surfaces consisting of polymer nanosheets were prepared by simple thermal polymerization of BME in an opal membrane. The thicknesses of the nanosheets were roughly constant, but their sizes (lengths and widths) and surface densities were highly variable and were related to the thickness (depth) of the silica opal membrane and the amount of BME solution applied.

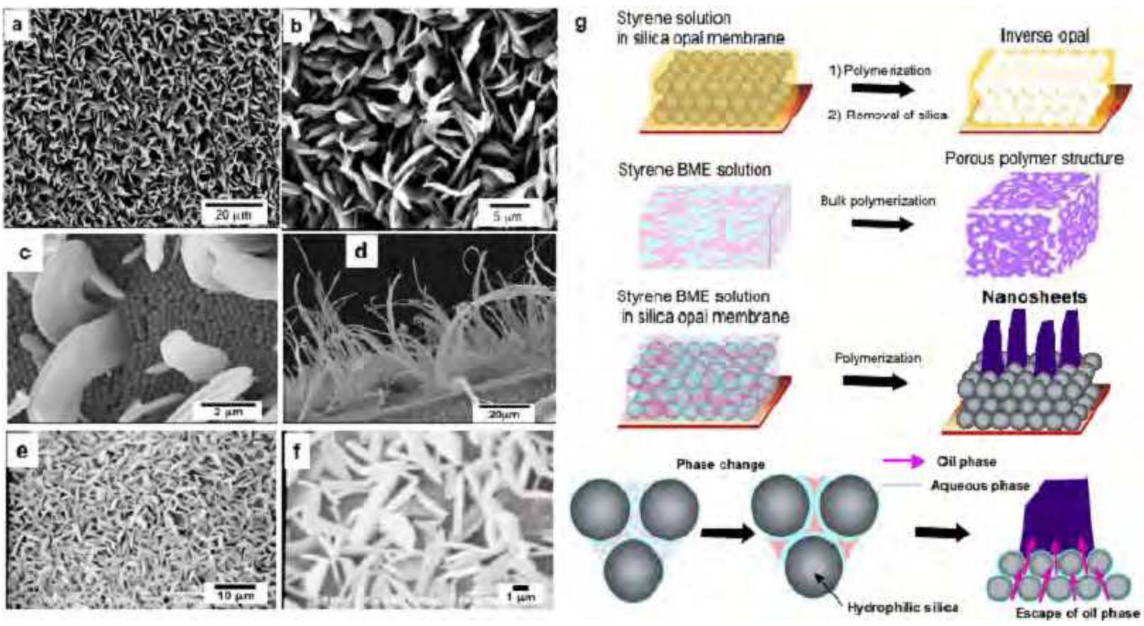

Fig. 7. Typical SEM images of PS (a–d) and PMMA (e and f) nanosheets prepared by polymerization of BME in silica gaps, and schematic representations (g) of the formation mechanism of nanosheets grown in the gaps of a silica opal membrane.[56]

These results prove that a combination of a regularly ordered "solid" microspace such as an opal membrane and the dynamic solution/solution structure of the ME, which can change in response to a variety of circumstances, has the potential for construction of hierarchical polymer structures by self-organization.

6. Conclusions

This chapter has introduced various unique polymer materials with controlled nanostructures based on polymerization or gelation of BMEs. Using bicontinuous solution structures in BMEs as a template, continuous porous materials and bicontinuous hybrid materials are prepared by polymerization or gelation in one side (water or oil phase) and in both sides, respectively. Similar structures can also be prepared by micro-phase separation of block copolymers and spinodal decomposition. Figure 8 summarizes the correlations among these three methods. The spinodal decomposition process is controlled kinetically, whereas micro-phase separation is completely thermodynamically controlled, with respect to the nature, shape, and length of each component. In the case of nanostructured polymer materials prepared from BMEs, the nanostructures are regulated both thermodynamically and kinetically. The solution structure of an ME is essentially ruled thermodynamically by the HLB. During the polymerization process, the structures of the polymers formed are controlled kinetically, as in spinodal decomposition, because the HLB is continuously changing as a result of polymer formation. The intentional regulation of competitive reactions between immobilization and phase separation allows us to control pore size or phase-separation size from several tens of nanometers to several microns.

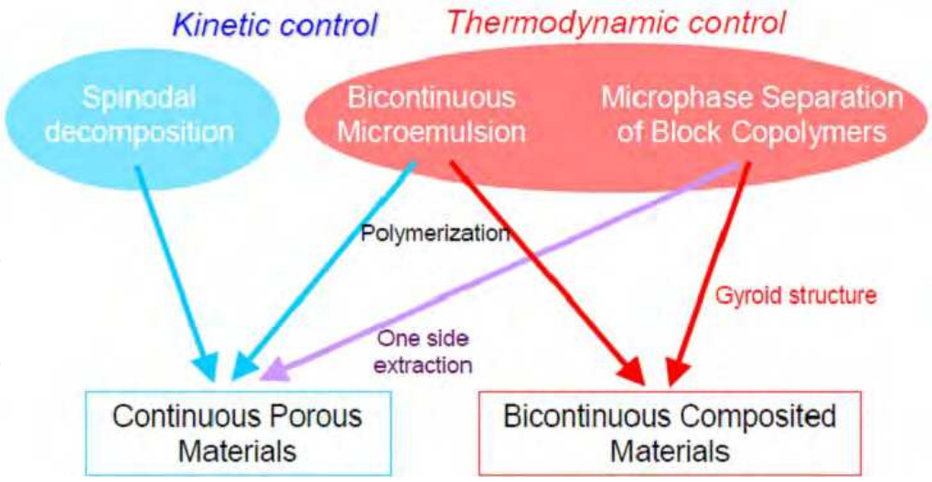

Fig. 8. Production of continuous porous materials and bicontinuous hybrid materials. The blue and red arrows (and areas) represent kinetically and thermodynamically controlled phenomena (or processes), respectively.

The structures of polymer products near a contacting surface change considerably. In particular, a BME is a precise well-balanced system, which can be easily deformed by changes in conditions. In other words, BMEs can produce a great diversity of hierarchical nanostructures by self-organization. Moreover, a lyotropic LC phase is used as a template instead of the BME. A lyotropic LC phase can be intentionally prepared from a BME with a relatively high surfactant-concentration. Frequently, changes in the HLB during polymerization induces a phase transition to a lyotropic LC phase, giving ribbon, tape, and plate structures. It will be possible to use these methods to produce highly advanced, polymer materials with hierarchical nanostructures, in a way similar to that found in living systems.

7. References

[1] Lovell P. A. & El-Aasser M. S. (1997). Emulsion Polymerisation and Emulsion Polymers, John Wiley and Sons (New York).
[2] Konno, M. Terunuma, Y. & Saito, S. (1991). J. Chem. Eng. Jpn. 24, 429-437.
[3] Tseng, C. M., Lu, Y. Y., El-Aasser, M. S. & Vanderhoff, J. W. (1986). J. Polym. Sci., Part A: Polym. Chem., 24, 2995-3007.
[4] Baines, F. L., Dionisio, S., Billingham, N. C. & Armes, S. P. (1996). Macromolecules, 29, 3096-3102.
[5] Minami, H., Yoshida, K. & Okubo, M. (2008). Macromol. Rapid Commun., 29, 567-572.
[6] Schmid, A., Fujii, S. & Armes, S. P. (2005). Langmuir, 21, 8103-8105.
[7] Dawkins, J. V., Neep, D. J. & Shaw, P. L. (1994) Polymer, 35, 5366-5368.
[8] Paine, A. J., Luymes, W. & McNulty, J. (1990). Macromolecules, 23, 3104-3109.
[9] Hong, J., Han, H., Hong, C. K. & Shim, S. E. (2008). J. Polym. Sci., Part A: Polym. Chem., 46, 2884-2890.
[10] Li, K. & Stover, H. D. H. (1993). J. Polym. Sci., Part A: Polym. Chem., 31, 3257-3263.
[11] Downey, J. S., Frank, R. S., Li, W.-H. & Stoever, H. D. H. (1999). Macromolecules, 32, 2838-2844.
[12] Nakanishi, K. (1997). J. Porous Mater., 4, 67-122.

[13] Hashimoto, T., Tsutsumi, K. & Funaki, Y. (1997). Langmuir, 13, 6869-6872.
[14] Ulbricht, M., Schuster, O., Ansorge, W., Ruetering, M. & Steiger, P. (2007). Separ. Purif. Tech., 57, 63-73.
[15] Kumar, A. & Srivastava, A. (2010). Nature Protocols, 5, 1737-1747.
[16] Jinnai, H., Hashimoto, T., Lee, D. & Chen, S.-H. (1997). Macromolecules, 30, 130-136.
[17] Hashimoto, T. (2005). Bull. Chem. Soc. Jpn., 78, 1-39.
[18] Haque, E. & Qutubuddin, S. (1988). J. Polym. Sci., Part C: Polym. Lett., 26, 429-432.
[19] Ryan, L. D. & Kaler, E. W. (1998). J. Phys. Chem. B, 102, 7549-7556.
[20] Sharma, S. C., Tsuchiya, K., Sakai, K., Sakai, H., Abe, M. & Miyahara, R. (2008). J. Oleo Sci., 57, 669-673.
[21] Ikeda, Y., Imae, T., Hao, J., Iida, M., Kitano, T. & Hisamatsu, N. (2000). Langmuir, 16, 7618-7623.
[22] Nagarajan, R. & Ruckenstein, E. (2000). Langmuir, 16, 6400-6415.
[23] Deen, G. R. & Gan, L. H., (2009) J. Polym. Sci., Part A: Polym. Chem., 47, 2059-2072.
[24] Gan, L. M., Chow, P. Y., Liu, Z., Han, M. & Quek, C. H. (2005). Chem. Commun., 4459–4461.
[25] Lim, T. H., Tham, M. P., Liu, Z., Hong, L. & Guo, B. (2007). J. Membr. Sci., 290, 146–152.
[26] Wang, L.-S., Chow, P.-Y., Phan, T.-T., Lim, I. J. & Yang, Y.-Y. (2006). Adv. Funct. Mater., 16, 1171–1178.
[27] Kawano, S., Kobayashi, D., Taguchi, S., Kunitake, M. & Nishimi, T. (2010). Macromolecules, 43, 473-479.
[28] (a) Osada, Y., Okuzaki, H. & Hori, H. (1992). Nature, 355, 242-244. (b) Holtz, J. H. & Asher, S. A. (1997). Nature, 389, 829-832. (c) Siegel, R. A. (1998). Nature, 394, 427-428. (d) Yoshida, R., Sakai, K., Okano, T. & Sakurai, Y. (1994). J. Biomater. Sci., Polym. Ed., 6, 585-598. (e) Hirose, M., Kwon, O. H., Yamato, M., Kikuchi, A. & Okano, T. (2000). Biomacromolecules, 1, 377-381.
[29] (a) Yang, W., Furukawa, H. & Gong, J. P. (2008). Adv. Mater., 20, 4499-4503. (b) Gong, J. P., Katsuyama, Y., Kurokawa, T. & Osada, Y. (2003). Adv. Mater., 15, 1155-1158.
[30] Haraguchi, K. & Takehisa, T. (2002). Adv. Mater., 14, 1120-1124.
[31] (a) Sakai, T., Murayama, H., Nagano, S., Takeoka, Y., Kidowaki, M., Ito, K. & Seki, T. (2007). Adv. Mater., 19, 2023-2025. (b) Okumura, Y. & Ito, K. (2001). Adv. Mater., 13, 485-487.
[32] Fukushima, T., Asaka, K., Kosaka, A. & Aida, T. (2005). Angew. Chem., Int. Ed., 44, 2410-2413.
[33] Sakata, S., Uchida, K., Kaetsu, I. & Kita, Y. (2007). Phys. Chem., 76, 733-737.
[34] Rees, G. D. & Robinson, B. H. (1993). Adv. Mater., 5, 608-619.
[35] (a) Hernandez-Barajas, J. & Hunkeler, D. J. (1995). Polym. Adv. Technol., 6, 509-517
(b) Dowding, P. J., Vincent, B. & Williams, E. (2000). J. Colloid Interface Sci., 221, 268-272.
[36] (a) Trickett, K. & Eastoe, J. (2008). Adv. Colloid Interface Sci., 144, 66-74. (b) Jadhav, K. R., Kadam, V. J. & Pisal, S. S. (2009). Current Drug Delivery, 6, 174-183. (c) Murdan, Sudaxshina (2005) Expert Opin. Drug Delivery, 2, 489-505.
[37] (a) Chen, H., Chang, X., Du, D., Li, J., Xu, H. & Yang, X. (2006). Int. J. Pharm., 315, 52-58. (b) Kreilgaard, M. (2001). Pharm. Res., 18, 367-373.
[38] Hirokawa, Y., Okamoto, T., Kimishima, K., Jinnai, H., Koizumi, S., Aizawa, K. & Hashimoto, T. (2008). Macromolecules, 41, 8210-8219.
[39] (2004). Advances in Polymer Science, Springer (Berlin and Heidelberg).

[40] Hirokawa, Y., Jinnai, H., Nishikawa, Y., Okamoto, T. & Hashimoto, T. (1999). Macromolecules, 32, 7093-7099.
[41] Kunitake, M., Murasaki, S., Yoshitake, S., Ohira, A., Taniguchi, I., Sakata, M. & Nishimi, T. (2005). Chem. Lett., 34, 1338-1339.
[42] Marckey, B. A., Texter, J. (1991). Electrochemistry in Colloid and Dispersions, Wiley-VCH (New York)
[43] Rusling, J. F. (2001). Pure Appl. Chem., 73, 1895-1905.
[44] Iwunze, M. O., Sucheta, A. & Rusling, J. F. (1990). Anal. Chem., 62, 644-649.
[45] Yoshitake, S., Ohira, A., Tominaga, M., Nishimi, T., Sakata, M., Hirayama, C. & Kunitake, M. (2002). Chem. Lett., 360-361.
[46] Kunitake, M., Murasaki, S., Yoshitake, S., Ohira, A., Taniguchi, I., Sakata, M. & Nishimi, T. (2005). Chem. Lett., 34, 1338-1339.
[47] Guéring, P. & Lindman, B. (1985). Langmuir, 1, 464-468.
[48] Makita, Y., Uemura, S., Miyanari, N., Kotegawa, T., Kawano, S., Nishimi, T., Tominaga, M., Nishiyama, K. & Kunitake, M. (2010). Chem. Lett., 39, 1152-1154.
[49] Zhou, X. L., Lee, L. T., Chen, S. H. & Strey, R. (1992). Phys. Rev. A, 46, 6479-6489.
[50] Zhou, X.-L. & Chen, S.-H. (1995). Phys. Rep., 257, 223-348.
[51] Olsson U. (2001). in Holmberg K., Handbook of Applied Surface and Colloid Chemistry, John Wiley & Sons, Chichester, 2, 333-356.
[52] Asakawa, K. & Hiraoka, T. (2002). Jpn. J. Appl. Phys., 41, 6112-6118.
[53] Schepelina, O. & Zharov, I. (2006). Langmuir, 22, 10523-10527.
[54] Rong, J. & Yang, Z. (2002). Macromol. Mater. Eng., 287, 11-15.
[55] Schroden, R. C., Al-Daous, M., Blanford, C. F. & Stein, A. (2002). Chem. Mater., 14, 3305-3315.
[56] Kawano, S., Nishi, S., Umeza, R. & Kunitake, M. (2009). Chem. Commun., 1688-1690.

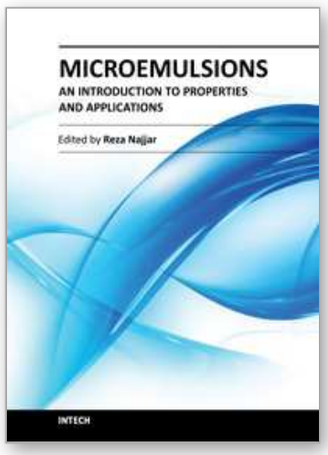

Microemulsions - An Introduction to Properties and Applications

Edited by Dr. Reza Najjar

ISBN 978-953-51-0247-2
Hard cover, 250 pages
Publisher InTech
Published online 16, March, 2012
Published in print edition March, 2012

The rapidly increasing number of applications for microemulsions has kept this relatively old topic still at the top point of research themes. This book provides an assessment of some issues influencing the characteristics and performance of the microemulsions, as well as their main types of applications. In chapter 1 a short introduction about the background, various aspects and applications of microemulsions is given. In Part 2 some experimental and modeling investigations on microstructure and phase behavior of these systems have been discussed. The last two parts of book is devoted to discussion on different types of microemulsion's applications, namely, use in drug delivery, vaccines, oil industry, preparation of nanostructured polymeric, metallic and metal oxides materials for different applications.

INTECH
open science | open minds

InTech Europe
University Campus STeP Ri
Slavka Krautzeka 83/A
51000 Rijeka, Croatia
Phone: +385 (51) 770 447
Fax: +385 (51) 686 166
www.intechopen.com

InTech China
Unit 405, Office Block, Hotel Equatorial Shanghai
No.65, Yan An Road (West), Shanghai, 200040, China
中国上海市延安西路65号上海国际贵都大饭店办公楼405单元
Phone: +86-21-62489820
Fax: +86-21-62489821

IntechOpen